

# PHYSICAL REVIEW B

## CONDENSED MATTER

THIRD SERIES, VOLUME 45, NUMBER 8

15 FEBRUARY 1992-II

### Relaxation and elastic anomalies in charge-density-wave conductors

Z. G. Xu and J. W. Brill

*Department of Physics and Astronomy, University of Kentucky, Lexington, Kentucky 40506-0055*

(Received 17 June 1991)

We have measured electric-field-dependent anomalies in the dynamic Young's and shear moduli and internal friction of the charge-density-wave (CDW) conductors TaS<sub>3</sub> and NbSe<sub>3</sub> at different mechanical frequencies  $\omega$  and field (i.e., current) frequencies  $f$ . For TaS<sub>3</sub> in a dc field, the anomalies decrease with increasing  $\omega$ , for  $\omega/2\pi > 300$  Hz; this decrease is independent of the amplitude of the resonance, indicating that we are remaining in a conventional elastic limit. For  $13 < \omega/2\pi < 300$  Hz, the anomalies are independent of  $\omega$ , implying that below the CDW depinning threshold, the average relaxation time  $> 10$  ms. Reversal of the field at frequency  $f$  introduces an internal friction peak at  $f = \omega/2\pi$  and a decrease in the internal friction at high  $f$  for both materials. These and previous results are discussed in terms of relaxational models.

#### I. INTRODUCTION

Various elastic properties of quasi-one-dimensional conductors have been observed to change significantly when their charge-density waves (CDW's) are depinned by an applied electric field.<sup>1</sup> The *dynamic* Young's<sup>2-5</sup> and shear<sup>5,6</sup> moduli decrease by as much as 20% and there are rapid changes in the internal friction at the depinning threshold field;<sup>1</sup> both increases and decreases in the internal friction have been observed, depending on the particular material and modulus.<sup>2-6</sup> Despite much experimental<sup>2-13</sup> and theoretical<sup>14-16</sup> work in the past few years, the physics governing these elastic changes remains poorly understood. In particular, it has proven difficult to account for the different signs observed for internal friction changes,<sup>5</sup> the relative magnitudes of the modulus and internal friction anomalies,<sup>2,5,6</sup> and their strain,<sup>9</sup> electric field (or CDW current),<sup>2,3</sup> and frequency<sup>11-13</sup> dependences. The Young's modulus anomalies in TaS<sub>3</sub> and NbSe<sub>3</sub> have been observed to decrease rapidly (as  $\omega^{-3/4}$ ) at frequencies above  $\sim 1$  kHz,<sup>11</sup> while no anomalies have been observed for TaS<sub>3</sub> in static measurements.<sup>13</sup>

Two approaches have been used most extensively in attempting to account for the elastic changes. Maki and Virosztek<sup>15</sup> (MV) have discussed the elastic anomalies in terms of the ability of the CDW to screen phonons; in this model the relative decrease in modulus with CDW depinning is proportional to the relevant electron-phonon coupling constant. On the other hand, Mozurkewich has developed a model in which the elastic anomalies are caused by relaxational changes in phase coherent

domains driven by the oscillating applied strains,<sup>16</sup> accounting in a relatively straightforward manner for the dependence of the anomalies on the frequency of the strain<sup>11,13</sup> as well as their dependence on the frequency of the applied electric field,<sup>10</sup> but not as readily for other details, as discussed below.

In this paper we describe results of some experiments meant to shed light on the question of the origin of the CDW elastic anomalies, in particular, the applicability of phase-relaxation models. The present experiments are extensions of those reported in Refs. 10 and 11, measuring the elastic anomalies at different strain<sup>11</sup> and current<sup>10</sup> frequencies. In particular, the strain-frequency range examined is extended (from 300 Hz) down to 13 Hz, and the current-frequency dependence is examined for a range of strain frequencies. As for most of the previous experiments,<sup>2-11</sup> measurements were made by studying mechanical (i.e., flexural and torsional) resonances in samples.

The plan of the paper is as follows. In Sec. II we briefly review past results. In Sec. III we discuss some of the empirical constraints on a relaxational model and reanalyze some previous data of ours<sup>2,11</sup> in terms of some of the ideas presented in Ref. 10. In Sec. IV we discuss experimental details. In Sec. V we present the results of measurements of the elastic anomalies in TaS<sub>3</sub> for dc fields at low-strain frequencies.<sup>17</sup> In Sec. VI we discuss the effects (for both NbSe<sub>3</sub> and TaS<sub>3</sub>) of varying the frequencies of both the electric field<sup>10</sup> and strain. In Sec. VII we digress to consider an explanation of the lack of a static anomaly<sup>13</sup> based on possibly different effects on a sliding CDW caused by bending versus uniaxially strain-

ing a crystal; this alternative is rejected for experimental reasons.<sup>17</sup> Finally in Sec. VIII, we briefly summarize our conclusions.

In this paper we will use  $f$  to denote the frequency of applied electric fields (i.e., current) and  $\omega/2\pi$  to denote the frequency of mechanical resonances.

## II. REVIEW

Most elastic measurements on CDW materials have been made using a vibrating reed technique,<sup>2,11</sup> in which a flexural resonance is excited in a crystal. If applied stresses are small, the Young's modulus  $Y$  is proportional to the square of the resonant frequency  $\omega$  so that  $\Delta Y/Y = 2\Delta\omega/\omega$ , and the internal friction is given by the reciprocal quality factor  $1/Q$ . For measurements of the shear modulus  $G$ , a stiff wire is attached to the center of the sample to act as an inertial element, and measurements are made of the torsional resonant frequency<sup>6</sup> ( $\omega \propto \sqrt{G}$ ) and reciprocal quality factor (internal friction). For applied electric field  $E > E_T$ , the threshold field at which the CDW becomes depinned and the resistivity starts to fall,<sup>1</sup> both moduli also start to decrease and the internal friction changes rapidly.<sup>2,6</sup>

Results for  $Y$  of TaS<sub>3</sub>,<sup>18</sup> the best studied material, at temperatures well below its CDW transition temperature (220 K), are shown in Fig. 6 of Ref. 2.  $Y$  typically decreases by 2% with increasing electric field, only saturating at  $E \sim 10E_T$ . The internal friction rapidly increases by  $\sim 2 \times 10^{-3}$ , peaks at  $E \sim 2E_T$ , and then usually falls slowly.<sup>2</sup> (The magnitude of the internal friction anomaly is somewhat sample dependent.) Sometimes a small hysteretic peak is observed in  $Y$  at  $E_T$ ,<sup>2,3</sup> otherwise,  $Y$  approaches its low field, pinned value as<sup>2</sup>  $Y(0, \omega) - Y(E, \omega) \simeq (E - E_T)^2$ . The shape of the anomalies in shear modulus and its internal friction are similar,<sup>6</sup> but the changes are typically an order of magnitude larger than for  $Y$  (Fig. 3 of Ref. 6).

Unlike TaS<sub>3</sub>, NbSe<sub>3</sub> has two CDW's that form independently (at 142 and 58 K) and can be independently depinned.<sup>19</sup> The elastic anomalies for the high-temperature CDW are typically an order of magnitude smaller than for TaS<sub>3</sub>, and those at the lower transition another order of magnitude smaller.<sup>5</sup> However, the magnitudes of the anomalies in NbSe<sub>3</sub> are very sample dependent, apparently varying with threshold field<sup>5</sup> (i.e., defect concentration<sup>1</sup>); in contrast, for TaS<sub>3</sub> the anomalies have been shown to be independent of defect concentration.<sup>8</sup> Another striking difference between the two materials is that for NbSe<sub>3</sub> the internal friction associated with the shear modulus, for both CDW's, and the Young's modulus, at the lower transition, decrease when the CDW becomes depinned.<sup>20,5</sup>

For both materials, the dependence of the Young's modulus anomalies on strain frequency (300 Hz to 100 kHz) was studied by doing measurements on higher flexural overtones.<sup>11</sup> While the shape of the anomalies (i.e., field dependence) is essentially independent of mode, their magnitudes fall roughly as  $\omega^{-3/4}$ . On the other hand, static measurements of  $Y$  of TaS<sub>3</sub>, made by measuring changes in uniaxial strain for a constant uniaxial

stress, indicate *no* variation in  $Y$  with field;<sup>13</sup> i.e.,  $|\Delta Y/Y| < 0.1\%$ . One of the motivations of the present research (Sec. V) was to examine the apparent inconsistency between these two works by extending our measurements to lower frequencies.

With the initial discovery of the Young's modulus anomalies in TaS<sub>3</sub>, it was suggested that they were due to the relaxation of CDW domains in the oscillating strain.<sup>2</sup> For discrete Debye relaxation processes of strengths  $F_K$  and relaxation times  $\tau_K$ ,

$$\begin{aligned} \operatorname{Re}[Y(E, \omega) - Y(0, \omega)] &= - \sum_K F_K / [1 + (\omega\tau_K)^2], \\ Y(0, \omega) / Q(E, \omega) &= \operatorname{Im}[Y(E, \omega)] \\ &= \sum_K F_K \omega\tau_K / [1 + (\omega\tau_K)^2]. \end{aligned} \quad (1)$$

For a single relaxation process, the internal friction peaks at  $\omega\tau = 1$ . Hence the results for TaS<sub>3</sub> suggest that the average relaxation time  $\tau \gg 1/\omega$  when the CDW is pinned, so that the measured modulus is unrelaxed. When the CDW slides,  $\tau$  decreases and the sample can relax. Obviously, in the static limit,<sup>13</sup> the modulus will always be relaxed and no anomalies are expected. Mozurkewich<sup>16</sup> explicitly considered the relaxation of phase coherent CDW domains. In the "weak-pinning" limit, the phase is coherent over an impurity-dependent "Lee-Rice" length,<sup>21</sup>  $L_{LR}$ . Mozurkewich showed that of the possible strain-dependent parameters which determine  $L_{LR}$ , the one most likely to account for the large, defect-independent anomalies in TaS<sub>3</sub>, is the CDW wave vector,<sup>16</sup> which implies a strain-dependent band structure. On the other hand, a strain-dependent CDW amplitude or stiffness leads to a smaller anomaly, proportional to the threshold field,<sup>16</sup> as observed in NbSe<sub>3</sub>.<sup>5</sup>

Recently, Jacobsen, Weissman, and Mozurkewich<sup>10</sup> (JWM) measured changes in the size of the Young's modulus anomalies in TaS<sub>3</sub> for square-wave electric fields above the threshold of variable frequency  $f$ . The anomalies initially increase with  $f$ , with the internal friction peaking at  $f \sim \omega/2\pi$  and the modulus anomaly peaking at  $f$  a few times greater than this;<sup>10</sup> both quantities decrease at high  $f$ .<sup>5,7,10</sup> JWM accounted for these features by assuming at least two relaxation processes, one with  $f$  controlling the average relaxation rate and the other with  $f$  controlling the relaxation strength.<sup>10</sup>

The most successful alternative approach was that of MV (Ref. 15); they considered the effect of CDW screening on phonons. They assumed that while the pinned CDW could not contribute to screening, the depinned could, so that the relative decrease in a modulus is proportional to the relevant electron-phonon coupling constant  $\lambda$ ; for phonon wave vector  $q \sim 0$ , this again implies a strain-dependent band structure.<sup>5,15</sup> This model accounts for the detailed field dependence of the modulus by assuming that the CDW is depinned heterogeneously, i.e., that there is a distribution of threshold fields. We pointed out that the model could also account for the threshold field dependence of the anomalies observed in NbSe<sub>3</sub> if the CDW pinning frequency were less than 1 GHz (Ref. 5); however, it is typically a few times greater

than this.<sup>1</sup> A surprising prediction of the MV model is that the internal friction should decrease when the CDW becomes depinned,<sup>15</sup> as is observed for most modes in NbSe<sub>3</sub> (Refs. 5 and 20); this result holds in the “collisionless” limit,  $\omega \ll Dq^2$  ( $D$  is the electron diffusion constant<sup>15</sup>) which is valid for all vibrating reed and torsional oscillator experiments.<sup>11</sup> For  $T \sim T_c$ ,

$$\Delta 1/Q \sim -\lambda(\omega/Dq^2), \quad (2)$$

so that  $\Delta 1/Q$  is less than the modulus change  $\lambda$ , and independent of frequency for flexural overtones, with  $\omega \sim q^2$ .<sup>11</sup> In fact, for NbSe<sub>3</sub>, the frequency dependence of  $\Delta 1/Q$  is not clear.<sup>11</sup>

The major failure of the MV model is its inability to account for the observed frequency dependence of the modulus anomalies. MV assume that the depinning anomalies should have the same frequency dependence as temperature-dependent changes observed for the pinned CDW at the transition temperature;<sup>15</sup> both should fall for large wave-vector modes, for which the phonon can still be screened by a pinned CDW.<sup>15</sup> (For flexural modes, this crossover frequency is  $\sim 40$  kHz.<sup>11</sup>) However, no frequency dependence was observed in the temperature dependence, while the depinning anomalies are strongly frequency dependent.<sup>11</sup> What is required to explain the disappearance of depinning anomalies at high  $\omega$  (or  $q$ ) is not a decrease of the pinned modulus with  $\omega$  but an increase of the depinned modulus.

### III. CONSTRAINTS ON RELAXATION MODELS

If the CDW elastic depinning anomalies are predominantly relaxational, the relaxation strengths must depend on uniaxial strain in the sample<sup>9</sup> as well as the current frequency.<sup>10</sup> New results on the latter will be discussed in Sec. VI. In this section we discuss constraints on relaxational models from previous results of the Young's modulus of TaS<sub>3</sub> in dc fields.<sup>2,11</sup>

Even for dc fields it was recognized that the Young's modulus anomaly could not be described by a single relaxation process, because experimentally the anomaly in  $1/Q$  is much smaller than that in  $Y$ . On the other hand,

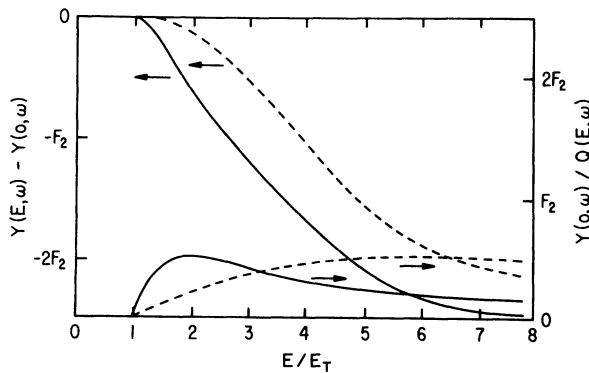


FIG. 1. Calculated Young's modulus and internal friction as a function of electric field for the relaxation processes given by Eq. (3). Solid curves,  $\omega = 1/\tau_0$ ; dashed curves,  $\omega = 5/\tau_0$ .

the internal friction anomaly is “faster” than the modulus anomaly so that at  $E \sim 2E_T$ , where  $1/Q$  peaks,  $\Delta Y/Y \sim -\Delta 1/Q$ ; see Fig. 6 of Ref. 2. Thus most of the “high-field” decrease of modulus has no associated internal friction; its relaxation strength must increase at fields for which  $\tau \ll 1/\omega$ .<sup>2</sup> Such was also suggested by Jericho and Simpson<sup>12</sup> to fit their ultrasonic data. The second relaxation process need not have a field-dependent relaxation strength, but its relaxation time should diverge at threshold as  $1/(E - E_T)$  to give the observed quadratic (linear) variations on field of the modulus (internal friction).<sup>2</sup>

In Fig. 1 we show calculated field dependences of modulus and internal friction, Eq. (1), with two processes,

$$\begin{aligned} \tau_1 &= \tau_0/1000, \\ \tau_2 &= \tau_0 E_T / (E - E_T), \\ F_1 &= 1.5 F_2 \tanh[(E/E_T - 1)^2/16], \\ F_2 &= \text{const}. \end{aligned} \quad (3)$$

The form of  $F_1$  was chosen to mimic the behavior observed at low frequencies,<sup>2</sup> e.g.,  $\omega = 1/\tau_0$ . However, at higher frequencies, the calculated anomalies move out to higher fields, but their magnitudes do not decrease, as shown. This is in striking contrast to the results of Ref. 11, in which it was shown that the anomalies decrease with frequency, but their shapes are frequency independent. A frequency-dependent shape is a necessary feature of any collection of discrete relaxation processes with relaxation times decreasing with increasing field.

In fact, the observed shape independence and approximate frequency power law of the Young's modulus anomaly,<sup>11</sup>

$$\begin{aligned} Y(0, \omega) - Y(E, \omega) &\sim A(E)/\omega^p \quad \text{with } p \sim \frac{3}{4}, \\ 1/Q(E, \omega) - 1/Q(0, \omega) &\sim B(E)W(\omega), \end{aligned} \quad (4)$$

implies a power-law distribution of relaxation strengths,  $F(\tau) \sim A(E)\tau^{p-1}$ ; however, this distribution is inconsistent with both the shape and magnitude of the internal friction anomaly.

Because of our lack of knowledge of  $F(\tau)$ , JWM took the alternative approach of plotting  $\Delta 1/Q = \text{Im}(\Delta Y/Y)$  vs  $\text{Re}(\Delta Y/Y)$  in a so-called “Cole-Cole” plot,<sup>10</sup> in such a plot, the average relaxation time can be considered an implicit parameter. For the sample and mode examined, they found that the complex modulus  $\tilde{Y}$  can be described by the equation

$$\Delta \tilde{Y}/Y(0, \omega) = -y/[1 + (i\omega\tau')^{1-\alpha}]^\beta, \quad (5)$$

where  $y$  is a real constant ( $y \ll 1$ ) and  $\tau'$  an effective time constant. Equation (5) is a generalization of a single Debye relaxation incorporating a distribution of relaxation times associated with a single process.<sup>22,23</sup> JWM found  $\alpha \sim 0.6$  and  $\beta \sim 1.35$ , similar to the values obtained for the frequency-dependent dielectric constant in the pinned state,<sup>22</sup> which suggests that similar barriers affecting CDW relaxation apply when the CDW is pinned and “sliding.”<sup>10</sup>

In view of this remarkable result, we replotted some of our previous results in Cole-Cole plots. In Fig. 2(a) are replotted the TaS<sub>3</sub> Young's modulus data of Ref. 2, Fig. 6(b) ( $\omega=1200/s$ ,  $T=96K$ ). As shown, the data are inconsistent with Eq. (5) using JWM's exponents; a better choice is  $\alpha=0.75$  and  $\beta=3$ . For the latter parameters, the calculated values of  $\tau'$ , which depend critically on the choice of parameters, are also shown. For these "fits," the normalized relaxation strength  $y$  is chosen (approximately) to align the high-field data. The fits are both sample and, as shown in Fig. 2(b), mode (frequency and/or wave vector) dependent. In Fig. 2(b) are shown Cole-Cole plots for several flexural modes of sample 2 of Ref. 11 (see Figs. 2 and 3 of Ref. 11). The modes seem to separate into two groups, which, however, are not correlated to frequency. We feel that one should not give too much significance to the fits of the elastic properties to Eq. (5) if the fitting parameters are themselves frequency dependent.

We conclude this section by mentioning NbSe<sub>3</sub>. For most modes, the internal friction decreases with depinning; sometimes a small peak in  $1/Q$  is also observed near threshold.<sup>5,20</sup> If one assumes that the relaxation time must decrease with depinning, this implies that  $\tau < 1/\omega$  already below threshold; i.e., only the "right half" of a Cole-Cole plot is available. Since NbSe<sub>3</sub> remains metallic in its CDW states,<sup>1,19</sup> it is not surprising that its relaxa-

tion times would be less than that of semiconducting<sup>1,18</sup> TaS<sub>3</sub>, although it is not clear why these times should depend strongly on mode. Alternatively, one might suppose  $\tau \rightarrow \infty$  in the pinned state (as for TaS<sub>3</sub>) but MV screening<sup>15</sup> may cause the decrease in internal friction when depinned [Eq. (2)]. If the strength of phase relaxation in NbSe<sub>3</sub> is threshold field dependent, as mentioned above, then for sufficiently high threshold field samples, one might expect to see an increase in internal friction with depinning.

#### IV. EXPERIMENTAL NOTES

TaS<sub>3</sub> and NbSe<sub>3</sub> crystals were grown by usual vapor transport techniques.<sup>18,19</sup> Crystals were typically  $10 \mu\text{m} \times 30 \mu\text{m} \times 4 \text{mm}$  in size. Measurements of the Young's and/or shear modulus and internal friction versus voltage (field) were made simultaneously with measurements of the resistance, in two-probe measurements.<sup>2,6,11</sup> Samples were suspended as cantilevers between two sapphire pads; electrical and mechanical contact was made to the ends of the sample with silver paint. Mechanical resonances were excited in the sample through the use of either capacitive<sup>2,6</sup> or piezoelectric<sup>11</sup> transducers, and the resonance also detected capacitively, using either a cryogenic microphone circuit<sup>2</sup> or helical resonator detector<sup>11</sup> driving a phase-lock loop.

As mentioned above, the Young's (shear) modulus is proportional to the square of the flexural (torsional) resonant frequency,  $\omega_y$  ( $\omega_G$ ), and the internal friction is given by the reciprocal quality factor, usually determined by monitoring the amplitude of the resonance. For shear modulus and low-frequency ( $\omega_y/2\pi < 1 \text{ kHz}$ ) Young's modulus experiments, a stiff wire "flag" was epoxied to the center of the sample to serve as an inertial element;<sup>6</sup> for large flags, the resonant frequencies  $\omega_y \propto \sqrt{Y/M}$  and  $\omega_G \propto \sqrt{G/I}$ , where  $M$  and  $I$  are the mass and moment of inertia of the flag. Thus by adding progressively larger flags, lower frequencies can be examined. For a "flagless" sample, several flexural overtones could be observed, and hence high-frequency (up to 100 kHz) measurements of the Young's modulus made.<sup>11</sup>

In Sec. VI we discuss measurements of the anomalies for square wave fields of variable frequency  $f$  ( $10 \text{ Hz} < f < 1 \text{ MHz}$ ). For these experiments, a function generator was kept at constant amplitude while the frequency was varied. At these frequencies, the reactance of the sample is much larger than its resistance, and it was also assumed that the resistive loading of the function generator by the sample was independent of frequency; the latter is important for NbSe<sub>3</sub> which remains metallic below its CDW transitions.<sup>1</sup>

For quantitative comparisons of the size of the Young's modulus anomaly for different mechanical frequencies, it is important that very small uniaxial stress ( $\sigma \ll [a/L]^2 Y$ , where  $\sigma$  is the stress,  $L$  the length, and  $a$  the thickness of the sample) be applied to the sample.<sup>2</sup> To accomplish this, one of the sapphire pads was attached to a piezoelectric transducer so that the sample could be pulled or bent. The point of zero stress was determined as described in Ref. 9. The application of

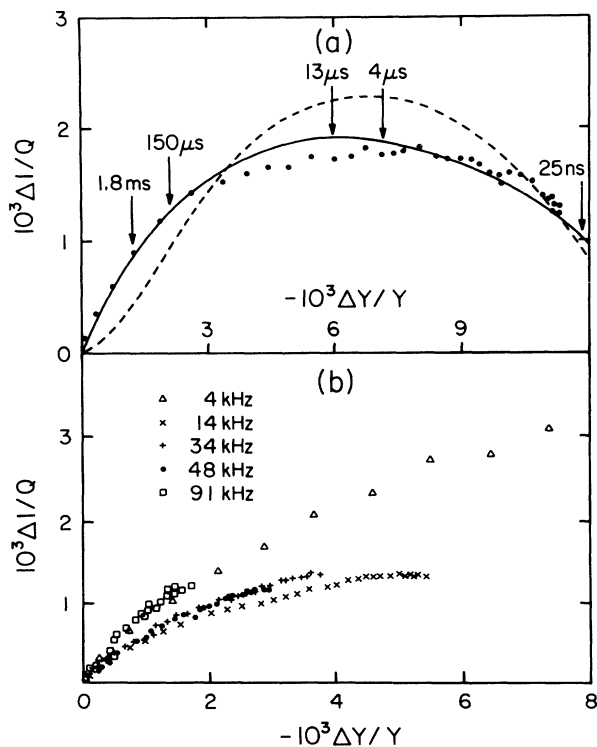


FIG. 2. (a) Cole-Cole plot for Young's modulus of TaS<sub>3</sub> sample of Ref. 2, Fig. 6(b) ( $\omega/2\pi=192 \text{ Hz}$ ). The solid curve is Eq. (5), with  $y=0.015$ ,  $\alpha=0.75$ ,  $\beta=3$ ; the times indicated are the resulting values of  $\tau'$ . The dashed curve is Eq. (5) with  $y=0.013$ ,  $\alpha=0.6$ ,  $\beta=1.35$ . (b) Cole-Cole plots for several flexural modes of TaS<sub>3</sub> sample 2 of Ref. 11.

stress also helps identify the torsional versus flexural modes, as the flexural resonant frequency depends strongly on stress whereas the torsional does not.<sup>9</sup> Keeping the sample straight also minimizes the amount of mixing between the two modes; however, this becomes increasingly more difficult as larger flags are attached to the sample.

All measurements were made isothermally ( $\Delta T < 0.05K$ ) at  $T = (100 \pm 5)$  K, where Joule heating at threshold is a minimum for both  $TaS_3$  and  $NbSe_3$  in its upper CDW state.<sup>1</sup> Measurements were made in a helium atmosphere of sufficient pressure that Joule heating was negligible at the fields used.<sup>5</sup>

### V. DEPINNING BY dc FIELDS

In Ref. 11, the mechanical frequency dependence ( $300 \text{ Hz} < \omega/2\pi < 100 \text{ kHz}$ ) of the Young's modulus anomalies was varied by studying flexural overtones. In this section we discuss measurements on  $TaS_3$  at lower frequencies, for both the shear and Young's moduli, made by putting progressively heavier flags on the sample.

Young's modulus data at three low frequencies for a single sample is shown in Fig. 3. The independence of shape on frequency [Eq. (4)] does not hold for the low-frequency experiments; e.g., for this sample a small maximum in  $Y$  is observed at  $E_T$  for 48 Hz and the peak in  $1/Q$  moves to lower fields with decreasing frequency. The latter effect is of course what would be expected from

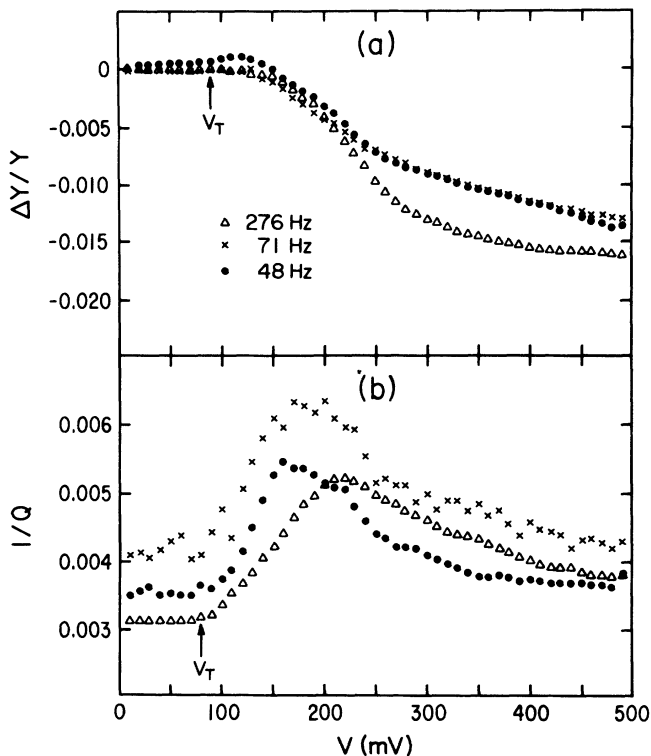


FIG. 3. (a) Change in Young's modulus [ $\Delta Y \equiv Y(E, \omega) - Y(0, \omega)$ ] and (b) internal friction for different low-frequency resonances of  $TaS_3$  vs voltage. The arrow indicates the threshold voltage.

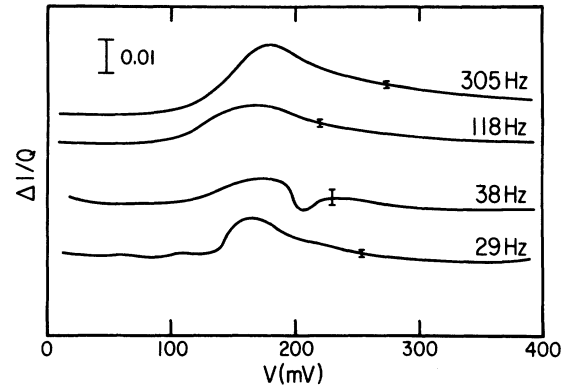


FIG. 4. Torsional internal friction vs voltage for a  $TaS_3$  sample at four frequencies. Vertical offsets are arbitrary. [ $\Delta 1/Q \equiv 1/Q(E, \omega) - 1/Q(0, \omega)$ ] (Ref. 17).

a simple relaxation model [Eq. (1) and Fig. 1] with the relaxation time diverging at  $E_T$ . In this case, the divergence is slower than we expect; if we associate the maximum in  $1/Q$  with  $\omega\tau = 1$ , we find  $\tau \sim 1/\sqrt{E - E_T}$ . Note, however, that this systematic shift was not observed for other samples; e.g., see Fig. 4.<sup>17</sup> We do not know if the shape dependence observed at low frequency is real or is an artifact introduced by "mode mixing," which is difficult to avoid as large flags can distort (e.g., twist) the sample.

In Fig. 5 we plot all our results on the frequency dependence of the depinning anomalies in the Young's and shear moduli and associated internal friction of  $TaS_3$ . For the modulus anomalies, we here define

$$|\Delta M/M| \equiv [M(0, \omega) - M(4E_T, \omega)]/M(0, \omega), \quad (6)$$

with  $M = Y$  or  $G$ ; the field  $4E_T$  is chosen for consistency and to avoid Joule heating problems.<sup>11</sup> The internal friction anomaly was similarly measured at  $4E_T$  when no peak was observed [e.g., Fig. 2(b)]; for samples for which a peak was observed (e.g., Figs. 3 and 4),

$$\Delta 1/Q \equiv 1/Q(\text{peak}) - 1/Q(E=0).$$

The new low-frequency data are shown together with the high-frequency data from Ref. 11. Clearly, the  $1/\omega^{3/4}$  behavior saturates at  $\omega/2\pi \sim 300$  Hz, and below this frequency, the anomalies become frequency independent. (Only for the sample shown by squares does the Young's modulus anomaly appear to be decreasing at the lowest frequency.) Again, the scatter in the data may reflect mode mixing. Thus, if the anomalies are relaxational in character, the average relaxation time in the pinned state must be greater than  $1/\omega(\text{minimum}) \sim 10$  ms.

Bhattacharya *et al.*<sup>24</sup> observed that the temperature dependence of the broad band noise (BBN) spectrum observed above threshold in  $TaS_3$  was related to that of the pinned ac conductivity, which, as JWM (Ref. 10) pointed out, is related to the complex Young's modulus anomaly. It is therefore not surprising that the frequency dependence of the BBN between 1 and 100 kHz has a similar power law ( $\omega^{-0.7}$ ) to the Young's modulus anomaly.<sup>24</sup> As discussed by JWM,<sup>10</sup> it seems that many low-

frequency phenomena may be governed by relaxation over similar barriers. Bhattacharya *et al.* suggested that the sliding state BBN reflects temporal fluctuations of Lee-Rice domains; the correlation with the pinned conductivity suggests that even for fields much greater than threshold, the CDW motion is “jerky,” with the CDW feeling its pinned barriers most of the time.<sup>24</sup> Similarly, the frequency dependence of  $\Delta Y/Y$  may be correlated with possible mechanical noise in the sliding state through a fluctuation-dissipation theorem. For this analogy to hold, the frequency dependence of  $\Delta Y$  should mainly be due to a frequency dependence in the pinned, rather than sliding, modulus. (Similarly, the ac conductivity in the sliding state is independent of frequency below 100 kHz.<sup>25</sup>) However, this interpretation (i.e.,  $\omega\langle\tau\rangle \ll 1$  for  $E > E_T$  and  $\omega\langle\tau\rangle \sim 1$  for  $E < E_T$ ) is inconsistent with a relaxational model for the internal friction; it would imply that the internal friction decreases when the CDW becomes depinned, which it does not for TaS<sub>3</sub>, and that  $\Delta 1/Q$  have a similar frequency dependence to  $\Delta Y/Y$ , which it does not [see Eq. (4)].

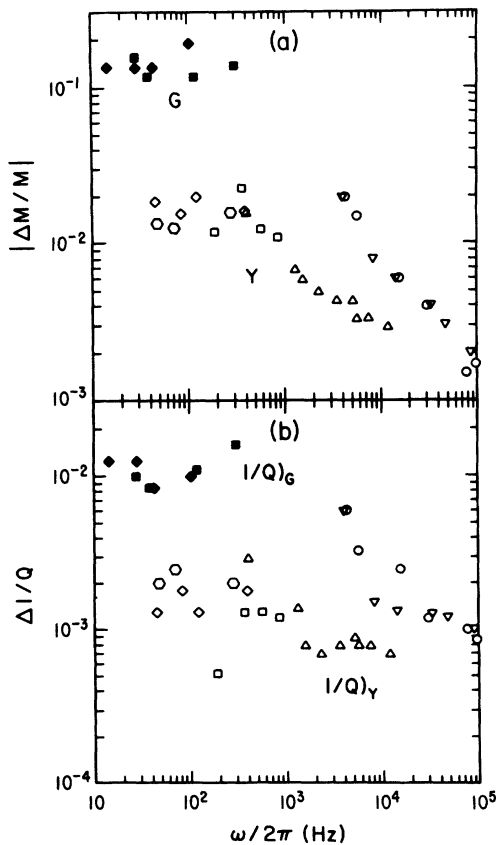


FIG. 5. (a) “Total” modulus and (b) internal friction anomalies (defined in text) for several samples of TaS<sub>3</sub> vs resonance frequency  $\omega$ . The different symbols are for different samples. Circles, triangles, and inverted triangles are the previous results (Ref. 11); hexagons, diamonds, and squares are the new results. Open symbols are for flexural modes and closed symbols are for torsional modes.

It may be significant that the frequency dependence of the modulus is observed for higher overtones (larger  $q$  modes), while no frequency dependence is observed for “weighted modes,” (with  $q \sim \pi/L = \text{const}$ ); i.e. the observed dependence may be a  $q$  dependence rather than an  $\omega$  dependence. The only calculated  $q$  dependence is that of MV,<sup>15</sup> which, as discussed in Sec. II, is inconsistent with the measured temperature dependence.<sup>11</sup>

## VI. DEPINNING BY ac (SQUARE-WAVE) FIELDS

JWM examined the changes in Young’s modulus and internal friction (for  $\omega/2\pi \sim 1$  kHz) of TaS<sub>3</sub> for square-wave voltages of variable frequency  $f$  and amplitude, which periodically switch the direction of CDW current and polarization.<sup>10</sup> For all amplitudes above threshold, they found that the internal friction peaked at  $f = \omega/2\pi$  and the modulus is a minimum for  $f$  a few times larger than this.<sup>10</sup> These results were interpreted in terms of two types of relaxation processes; switching opens new relaxation channels, with relaxation time  $= 1/2\pi f$ , while switching at a high frequency suppresses (i.e., decreases the relaxation strength of) the relaxation associated with dc depinning, e.g., by closing relaxation channels with  $\tau > 1/2\pi f$ .<sup>10,26</sup> It was therefore of interest to also vary  $\omega$  in such measurements. This we did by studying overtones as well as weighted samples at several fields.

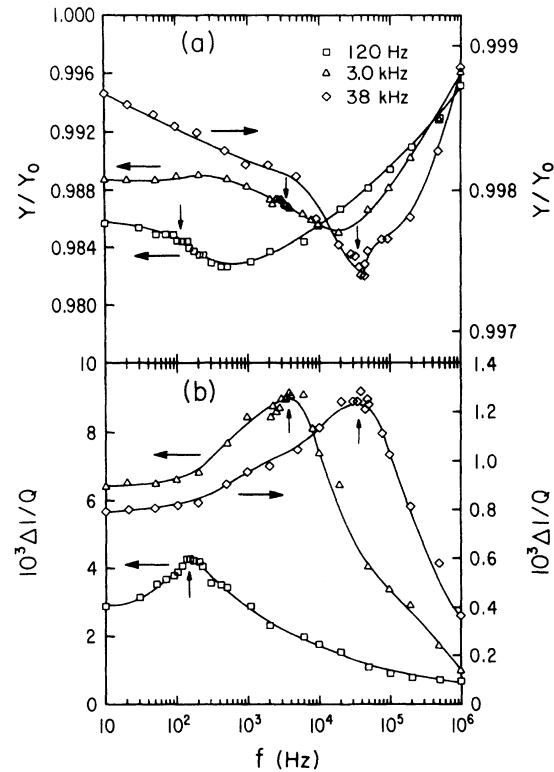


FIG. 6. (a) Young’s modulus and (b) change in internal friction (b) vs field-switching frequency, measured for a sample of TaS<sub>3</sub> at a field of  $2.5E_T$  for three flexural resonant frequencies, indicated by the vertical arrows. [ $\Delta 1/Q \equiv 1/Q(E, \omega, f) - 1/Q(0, \omega)$ ;  $1/Q(0, \omega) = (1-2) \times 10^{-3}$  for all three modes.] The curves are guides to the eye.

Representative results for a TaS<sub>3</sub> sample at fixed field ( $E \sim 2.5E_T$ ) are shown in Fig. 6; data at 3 kHz (unweighted fundamental), 38 kHz (third overtone), and 120 Hz (weighted sample) are shown. Note the different scales used for the 38-kHz data. The most important result is that the internal friction peaks at  $f = \omega/2\pi$  for all  $\omega$ , as predicted by JWM.<sup>10</sup> Also as they observe, the peak is asymmetric, with larger internal friction at small  $f$  than large. The structure in modulus also moves out to high  $f$  as  $\omega$  increases, but these changes are less well defined. For some voltages and modes,  $Y$  has a minimum at  $f \sim 5\omega/2\pi$ , as JWM observe;<sup>10</sup> in other cases (e.g., Fig. 6,  $\omega/2\pi = 38$  kHz),  $Y$  has a minimum much closer to  $\omega/2\pi$ . These effects are observed for all samples and fields greater than threshold, but the shapes and magnitudes of the  $f$ -dependent features vary. The depth of the minimum in modulus for  $f$  near  $\omega/2\pi$  is generally comparable to the height of the peak in  $1/Q$ , consistent with a relaxation process with  $\tau = 1/2\pi f$ . The anomalies disappear at high  $f$ , presumably as relaxation channels [e.g., those associated with  $F_1$  in Eq. (10)] close.<sup>10</sup> At dc and low  $f$ , there must be a large distribution of relaxation times, overlapping  $1/\omega$  for all modes, but (for this sam-

ple) with its greatest weight near  $50 \mu\text{s}$  (i.e., at the 3-kHz mode).

It was also of interest to measure  $f$ -dependent elastic changes in NbSe<sub>3</sub>, in view of the decrease in internal friction associated with the shear modulus.<sup>5</sup> In analogy to TaS<sub>3</sub>, one can imagine two very different results: (i) if the "anomalies" are maximized at  $f = \omega/2\pi$ , the internal friction for the shear mode should have a *minimum* here; (ii) if there is a relaxation process with  $\tau = 1/2\pi f$ , the internal friction for the shear mode should have a *maximum* at  $\omega/2\pi$ .

Results for both shear and Young's moduli of a crystal of NbSe<sub>3</sub> in its upper CDW state, for  $E = 1.7E_T$ , are shown in Fig. 7. For the Young's modulus [Fig. 7(a)], the results are similar to TaS<sub>3</sub>; there is a peak in  $1/Q$  at  $f = \omega/2\pi$  and minimum in  $Y$  at a frequency a few times higher than this.<sup>27</sup> The anomalies are disappearing at high switching frequency.

For the shear mode [Fig. 7(b)], there is also a broad *maximum* in  $1/Q$  at  $\omega/2\pi$ ,<sup>27</sup> i.e., case (ii) holds, with a modulus minimum at a frequency an order of magnitude above this. For this sample, in fact, the  $1/Q$  peak is sufficiently large that  $\Delta 1/Q$  becomes positive near the peak. At high  $f$ , the modulus anomaly is decreasing, as previously noted.<sup>5</sup> The internal friction again goes to a minimum at high  $f$ , so that the difference in internal friction with that at zero field is a *maximum*. These results imply, as for TaS<sub>3</sub>,<sup>10</sup> that at high  $f$  the modulus is becoming unrelaxed, not by an increase in  $\tau$ , but by a decrease in the number of relaxation channels available. These channels can even be closed somewhat by high-frequency switching voltages below threshold, as also shown in the figure, but low-frequency subthreshold switching increases the internal friction; subthreshold softening for dc fields was previously noted in Ref. 5.

## VII. FLEXURAL VERSUS UNIAXIAL STRAIN

A difference between the static<sup>13</sup> and dynamic<sup>1-12</sup> measurements of changes in the Young's modulus with dc field is that the former was made by uniaxial straining the sample, whereas most of the latter were made by studying changes in *flexural* resonant frequencies. (The only exception is the 10-MHz ultrasonic propagation measurement of Jericho and Simpson,<sup>12</sup> at this high frequency, the anomalies are comparable to the static upper limit.) In this section we discuss possible differences, other than the frequency, in the Young's modulus as measured by the two techniques.<sup>17</sup>

The Young's modulus is of course defined as the uniaxial stress divided by the uniaxial strain, which is what is directly measured in Ref. 13. The bending modulus, which governs flexural resonances, equals the Young's modulus if (i) the shear modulus is sufficiently large,  $G \gg (a/L)^2 Y$ , where  $L$  and  $a$  are the length and thickness, (ii) the sample cross section is symmetric, and (iii) the strains are everywhere small.<sup>28</sup> For the thin crystals of TaS<sub>3</sub> and NbSe<sub>3</sub> (i) holds.<sup>6</sup> Measurements on asymmetric samples may give rise to much of the observed

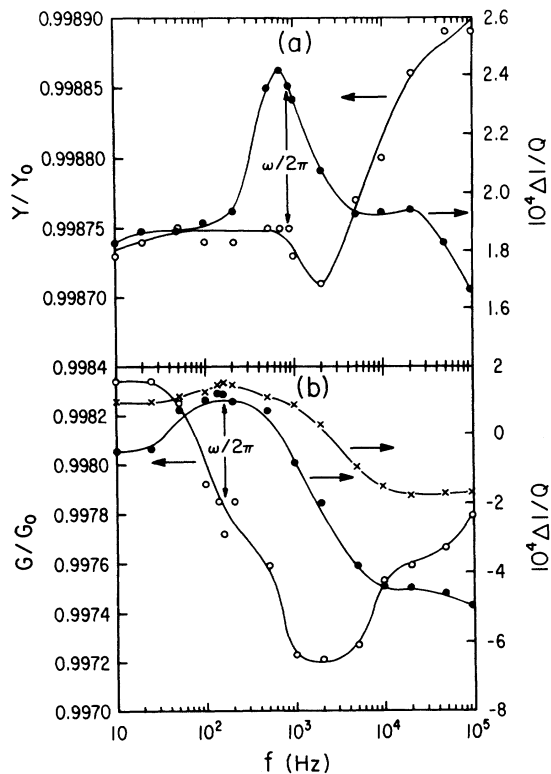


FIG. 7. (a) Young's modulus (open circles) and change in internal friction (closed circles) for a NbSe<sub>3</sub> sample with flexural resonant frequency of 790 Hz at a field of  $1.7E_T$ , as a function of field-switching frequency. [ $\Delta 1/Q \equiv 1/Q(E, \omega, f) - 1/Q(0, \omega)$ , with  $1/Q(0, \omega) = 2.0 \times 10^{-3}$ .] (b) Shear modulus (open circles) and change in internal friction (closed circles) for torsional resonant frequency of 160 Hz at a field of  $1.7E_T$ . Also shown is the change in internal friction (crosses) at  $E = E_T/2$ . [ $1/Q(0, \omega) = 5.8 \times 10^{-3}$ .] The curves are guides to the eye.

sample dependence of the flexural anomalies, especially in view of the large anomaly in shear modulus (i.e., there may be some mode mixing) but the magnitude of the ( $\omega/2\pi < 1$  kHz) flexural anomalies in TaS<sub>3</sub> is much too reproducible to be attributed mostly to asymmetry. Finally, care is generally taken in the flexural measurements to assure that the *lattice* strains are small (usually  $< 10^{-5}$ ).<sup>2</sup>

Regarding (iii) however, it is not necessarily true that strains in the *superlattice* associated with the CDW are small when bending the sample. A convenient measure of the strain in the superlattice is  $\nabla\phi$ , where  $\phi$  is the local CDW phase. When bending a reed in the  $x$ - $z$  plane, the uniaxial lattice strain  $\epsilon \equiv \epsilon_{zz}$  (taking the  $z$  axis along the length of the reed) varies slowly along the length of the sample and, rapidly across its thickness;  $d\epsilon/dx \sim 2\epsilon_{\max}/a$ . It has been shown that the CDW velocity ( $\propto d\phi/dt$ ) varies considerably with uniaxial strain;<sup>29</sup> hence there must be large oscillating phase gradients. These may be localized at defects or between phase-coherent Lee-Rice domains,<sup>21</sup> rather than distributed throughout the sample. Hence a crystal with a sliding CDW may provide a unique situation where the usual assumptions of elasticity theory<sup>28</sup> break down, giving rise to different Young's moduli as measured in flexural versus uniaxial strain experiments.

The most obvious experimental test of this possibility would be to measure static bending strain for fixed stress as a function of field. However, there is an indirect test we can make with our present system. For an oscillating sample, the transverse phase gradients develop over half an oscillation period so the local phase gradients will be proportional to  $\epsilon_{\max}/\omega$ . In fact, this may be the cause of the inverse-frequency dependence observed for flexural overtones; similarly, the depinning anomalies should then be amplitude dependent. While it was established from their initial discovery<sup>2</sup> that anomalies observed for fundamental resonances were amplitude independent, the  $\omega$  independence of the anomaly at low frequencies (Fig. 5) suggests that here the dependence of the modulus on phase gradients ( $\epsilon_{\max}/\omega$ ) has saturated. On the other

hand, the expected  $\epsilon_{\max}/\omega$  dependence suggests that the (saturated) low-frequency value of the anomaly should be recoverable at high frequencies by increasing the amplitude.

We therefore measured the amplitude dependence of the Young's modulus anomalies for high-frequency overtones of several samples of TaS<sub>3</sub> by varying the voltage applied to the piezoelectric driving the sample. (For previous experiments, the small signals observed for higher overtones had limited the range over which we limited this voltage.<sup>11</sup>) Typical results are shown in Fig. 8. For this sample, measurements were made on the third overtone at 38 kHz, for which the total Young's modulus anomaly is 30% of that of the fundamental (3 kHz). In no case was any significant amplitude dependence observed, apparently ruling out this novel explanation. However, static measurements of the bending and shear moduli are still desirable.

## VIII. CONCLUSIONS

The results of all the elastic measurements presented here can be interpreted in terms of relaxation, e.g., of CDW phase configurations, in the oscillating strains.<sup>16</sup> For TaS<sub>3</sub>, the relaxation strength is probably determined by the strain dependence of the CDW wave vector,<sup>16</sup> while the smaller anomalies in NbSe<sub>3</sub> may be governed by strain-dependent CDW amplitude and/or stiffness. As discussed in Sec. III, a very large distribution of relaxation time is required to understand the effects in a dc field, however, and this distribution cannot meaningfully be parametrized in terms of the generalized Debye process, Eq. (5). For TaS<sub>3</sub>, that the anomalies appear to saturate at mechanical frequencies as low as 13 Hz (Fig. 5) implies that in the pinned state,  $\langle \tau \rangle > 10$  ms. For NbSe<sub>3</sub>, very different pinned relaxation times would be required for torsional versus flexural strains to explain the different signs of the internal friction anomalies. Alternatively, MV screening<sup>15</sup> may have a large effect on the internal friction for NbSe<sub>3</sub>.

The distribution of relaxation times and strengths is greatly affected by the rate of switching the polarity of the field  $f$ . In particular, for TaS<sub>3</sub> a strong fast relaxation process which develops for fields above threshold is suppressed by rapid switching. New relaxation channels, with  $\tau = 1/2\pi f$ , open; for the shear mode in NbSe<sub>3</sub>, these processes can be sufficiently strong that they reverse the sign of the internal friction change.

While the main features of the anomalies may be qualitatively modeled in terms of relaxation processes, a detailed understanding of the complete mode- $\omega$ - $f$ - $E$  dependence of the elastic anomalies is illusive. There are striking, but incomplete, correlations between the elastic and electronic properties. In view of strong sample dependences, it will be very useful to compare experiments on a number of properties on the same sample, as has been started by JWM.<sup>10</sup>

The (more rapid) changes in elastic properties caused

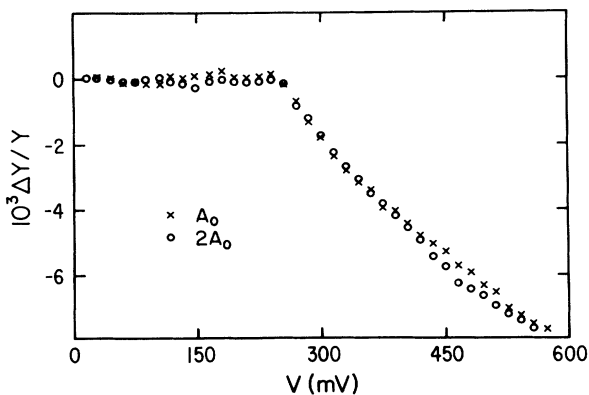


FIG. 8. Change in Young's modulus [ $\Delta Y \equiv Y(E, \omega) - Y(0, \omega)$ ] vs voltage at two drive amplitudes for a 38-kHz flexural overtone of TaS<sub>3</sub>.



by screening<sup>15</sup> should of course add to those due to slower relaxations, but, except possibly in the internal friction of NbSe<sub>3</sub>, they may be masked by them. Screening contributions to the elastic anomalies may be more discernible in either static or ultrasonic (i.e.,  $\omega\tau \ll 1$  or  $\omega\tau \gg 1$ ) measurements. Band-structure calculation giving the strain dependence of the Fermi surface and  $\lambda$  ( $q=0$ ) are obviously desirable.

#### ACKNOWLEDGMENTS

We are indebted to George Mozurkewich and Ron Jacobsen for many discussions of both their results and ours. We also thank Guy Lehman, Kazumi Maki, Malcolm Skove, Terry Tritt, Mike Weissman, and Xiaodong Xiang. This research was supported in part by National Science Foundation Grant No. DMR-89-15440.

- 
- <sup>1</sup>For a review of CDW depinning, see G. Gruner, *Rev. Mod. Phys.* **60**, 1129 (1988).
- <sup>2</sup>J. W. Brill, W. Roark, and G. Minton, *Phys. Rev. B* **33**, 6831 (1986).
- <sup>3</sup>R. L. Jacobsen and G. Mozurkewich, *Phys. Rev. B* **42**, 2778 (1990).
- <sup>4</sup>A. Suzuki, H. Mizubayashi, and S. Okuda, *J. Phys. Soc. Jpn.* **57**, 4322 (1988).
- <sup>5</sup>X.-D. Xiang and J. W. Brill, *Phys. Rev. B* **39**, 1290 (1989).
- <sup>6</sup>X.-D. Xiang and J. W. Brill, *Phys. Rev. B* **36**, 2969 (1987).
- <sup>7</sup>L. C. Bourne and A. Zettl, *Phys. Rev. B* **36**, 2626 (1987).
- <sup>8</sup>R. L. Jacobsen and G. Mozurkewich, *Phys. Rev. B* **39**, 10913 (1989).
- <sup>9</sup>Z. G. Xu and J. W. Brill, *Phys. Rev. B* **43**, 11037 (1991).
- <sup>10</sup>R. L. Jacobsen, M. B. Weissman, and G. Mozurkewich, *Phys. Rev. B* **43**, 13198 (1991).
- <sup>11</sup>X.-D. Xiang and J. W. Brill, *Phys. Rev. Lett.* **63**, 1853 (1989).
- <sup>12</sup>M. H. Jericho and A. M. Simpson, *Phys. Rev. B* **34**, 1116 (1986).
- <sup>13</sup>T. M. Tritt, M. J. Skove, and A. C. Ehrlich, *Phys. Rev. B* **43**, 9972 (1991).
- <sup>14</sup>L. Sneddon, *Phys. Rev. Lett.* **56**, 1194 (1986); R. Zeyher, *ibid.* **61**, 1009 (1988); A. S. Rozhavsky, Yu. S. Kivshar, and A. V. Nedzvetsky, *Phys. Rev. B* **40**, 4168 (1989).
- <sup>15</sup>K. Maki and A. Virosztek, *Phys. Rev. B* **36**, 2910 (1987); A. Virosztek and K. Maki, *ibid.* **41**, 7055 (1990).
- <sup>16</sup>G. Mozurkewich, *Phys. Rev. B* **42**, 11183 (1990).
- <sup>17</sup>A preliminary report of some of these results was presented in J. W. Brill and Z. G. Xu, Proceedings of the International Conference on Science and Technology of Synthetic Metals, Tubingen, 1990 [*Synth. Met.* **43**, 3787 (1991)].
- <sup>18</sup>T. Sambongi, K. Tsutsumi, Y. Shiozaki, Y. Yamamoto, K. Yamaya, and Y. Abe, *Solid State Commun.* **22**, (1977).
- <sup>19</sup>P. Monceau, N. P. Ong, A. M. Portis, A. Meerschaut, and J. Rouxel, *Phys. Rev. Lett.* **37**, 602 (1976).
- <sup>20</sup>For some samples, decreases in internal friction with CDW depinning are observed for all modes. The correlation of the sign of the internal friction change with other properties is under current investigation.
- <sup>21</sup>P. A. Lee and T. M. Rice, *Phys. Rev. B* **19**, 3970 (1979).
- <sup>22</sup>R. J. Cava, R. M. Fleming, R. G. Dunn, and E. A. Rietman, *Phys. Rev. B* **31**, 8325 (1985).
- <sup>23</sup>S. Havriliak and S. Negami, *J. Polymer Sci.* **C14**, 99 (1966).
- <sup>24</sup>S. Bhattacharya, J. P. Stokes, M. J. Higgins, and M. O. Robbins, *Phys. Rev. B* **40**, 5826 (1989).
- <sup>25</sup>S. Bhattacharya, J. P. Stokes, M. J. Higgins, and M. O. Robbins, *Phys. Rev. B* **43**, 1835 (1991).
- <sup>26</sup>Ronald L. Jacobsen, Ph.D. thesis, University of Illinois, 1991.
- <sup>27</sup>For another sample, the  $1/Q$  peaks coincide with the modulus minima at frequencies above  $\omega/2\pi$ .
- <sup>28</sup>S. Timoshenko, D. H. Young, and W. Weaver, Jr., *Vibration Problems in Engineering*, 4th ed. (Wiley, New York, 1971).
- <sup>29</sup>V. B. Preobrazhensky and A. N. Taldenkov, *Synth. Met.* **29**, F313 (1989); T. A. Davis, W. Schaffer, M. J. Skove, and E. P. Stillwell, *Phys. Rev. B* **39**, 10094 (1989).